Wedged multilayer Laue lens

Ray Conley,[1,a)] Chian Liu,[1] Jun Qian,[1] Cameron M. Kewish,[1] Albert T. Macrander,[1] Hanfei Yan,[1,2] Hyon Chol Kang,[2,3] Jörg Maser,[1,2] and G. Brian Stephenson[2,3]
[1]*X-ray Science Division, Argonne National Laboratory, Argonne, Illinois 60439, USA*
[2]*Center for Nanoscale Materials, Argonne National Laboratory, Argonne, Illinois 60439, USA*
[3]*Materials Science Division, Argonne National Laboratory, Argonne, Illinois 60439, USA*

(Received 18 January 2008; accepted 14 April 2008; published online 14 May 2008)

A multilayer Laue lens (MLL) is an x-ray focusing optic fabricated from a multilayer structure consisting of thousands of layers of two different materials produced by thin-film deposition. The sequence of layer thicknesses is controlled to satisfy the Fresnel zone plate law and the multilayer is sectioned to form the optic. An improved MLL geometry can be created by growing each layer with an in-plane thickness gradient to form a wedge, so that every interface makes the correct angle with the incident beam for symmetric Bragg diffraction. The ultimate hard x-ray focusing performance of a wedged MLL has been predicted to be significantly better than that of a nonwedged MLL, giving subnanometer resolution with high efficiency. Here, we describe a method to deposit the multilayer structure needed for an ideal wedged MLL and report our initial deposition results to produce these structures. © *2008 American Institute of Physics.*
[DOI: 10.1063/1.2924209]

Work is steadily progressing to push the limit for x-ray focusing to smaller length scales. Kirkpatrick–Baez mirrors producing spot sizes much smaller than 1 μm are common in the synchrotron community, with some results in the tens of nanometer range.[1,2] Adiabatically focusing compound refractive lenses can, in theory, produce 2 nm spot sizes,[3] although there remains, to date, no practical way to produce these optics with the perfection required. Diffractive optics such as the multilayer Laue lens (MLL) show promise for focusing to less than 1 nm with good efficiency.[4–7] The MLL is a type of zone plate fabricated by sectioning a multilayer to allow illumination in transmission (Laue) geometry. The multilayer sectioning process[8] can produce a much larger aspect ratio (zone depth to width ratio) than the conventional photolithographic process for zone plates, which is required for high efficiency focusing of hard x-rays to nanometer-scale sizes.

As shown in Fig. 1(b), four different geometries of the layers in a MLL have been considered in simulations:[4–7] flat, tilted, wedged, and curved. The layers in the flat or tilted MLL geometries have uniform in-plane thickness, so that the interfaces in each half are parallel, while the layers in the wedged or curved MLL geometries have an in-plane thickness gradient, so that the angle of each interface varies. Simulations show that flat or tilted MLLs with sufficient section depth to achieve high diffraction efficiency have a lower focal limit of ~5 nm imposed by dynamical diffraction effects.[5,7] This is due to the fact that only one region of the optic satisfies the Bragg condition and thereby diffracts strongly and in phase; i.e., only a fraction of the MLL contributes constructively to the focusing. In other words, the effective numerical aperture (NA) of flat or tilted MLLs is limited due to deviation from the Bragg condition. By incorporating wedging into every layer so that all layers make the correct local Bragg angle, we can increase not only the effective NA but also the integrated efficiency.[5] Theoretically, it is possible to achieve a focal size below 1 nm with over 50% efficiency by using a wedged MLL.[4–7] To date, only flat and tilted MLL geometries have been investigated experimentally,[5] since the precise control of the layer thickness sequence required is simplest to produce for uniform thickness layers. Here, we report a method and initial results for deposition of this next generation of nanofocusing optics for hard x-rays, the wedged MLL (wMLL), by using the rotary deposition system[9] in the Mirror Laboratory at the Advanced Photon Source.

The ideal curved MLL geometry for focusing a plane wave has layers forming confocal parabolic zones satisfying the relation[7]

$$x_n^2 = n\lambda(f_0 - z) + \frac{n^2\lambda^2}{4}, \tag{1}$$

where x_n is the distance from the optical axis to the outer edge of the nth zone, z is the distance along the optical axis measured from the upstream side of the optic, λ is the wavelength, and f_0 is the focal length measured from $z=0$. For the MLL sizes and focal lengths considered here (e.g., $\lambda \sim 0.01-0.03$ nm, $f_0 \sim 1-3$ mm, maximum $n \sim 3000$), the second term is negligible. This gives

$$x_n \approx a(z)(n\lambda f_0)^{1/2}, \tag{2}$$

$$a(z) = (1 - z/f_0)^{1/2}. \tag{3}$$

Thus, the positions of all interfaces and the thicknesses of all zones are scaled down as z increases by the same factor $a(z)$, independent of n. A multilayer having the appropriate internal structure can be produced by introducing a gradient in the deposition rate in the in-plane (z) direction that remains constant in time as all of the zones are deposited.

[a)]Author to whom correspondence should be addressed. Electronic mail: rconley@aps.anl.gov.

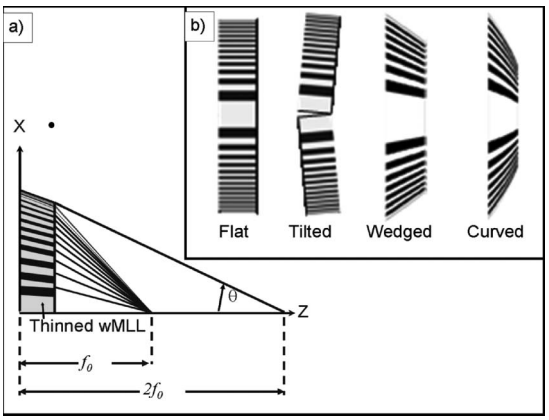

FIG. 1. (a) Diagram of a wedged MLL showing the progressively increasing layer tilt required to satisfy the Bragg condition at all positions along the x axis. The geometrical intersection of all the layers with the z axis occurs at twice the focal length, measured from the upstream face of the wMLL. (b) Four different types of multilayer Laue lens: flat, tilted, wedged, and curved.

The depth of the optic required for high efficiency at hard x-ray wavelengths (e.g., depths of 0.01–0.03 mm) is typically small compared to the focal length f_0. Thus, the gradient within the optic is approximately linear,

$$a(z) \approx \left(1 - \frac{z}{2f_0}\right). \tag{4}$$

This is the wedged MLL geometry,[7] in which each interface is flat but makes an angle with respect to the optical axis proportional to x_n. The extensions of all the interfaces intersect the optical axis at the same point at distance $z=2f_0$. The optimum amplitude for the deposition rate gradient $-2f_0^{-1}$ should be matched to the focal length of the layer sequence $x_n=(n\lambda f_0)^{1/2}$ at $z=0$. Note, however, that since the layer sequence depends on the product λf_0 rather than simply f_0, any gradient will match for some wavelength λ. Thus, several wedged MLL sections can be cut from a large area multilayer produced with a lateral gradient in deposition rate, but the optimum wavelength for each section may differ depending on the deposition rate distribution in z.

We investigated the deposition of high-precision multilayers for wMLL structures by using in-plane deposition rate gradients. The rotary deposition system used consists of a 0.76 m diameter, 0.34 m tall chamber with two 76.2 mm diameter circular magnetrons mounted sideways and sputtering toward the center of the chamber. Two horizontally opposed magnetrons are mounted sideways so that flakes from accumulated film growth fall down and away from the target, minimizing the possibility of disrupting the sputtering process. The sputtering guns are surrounded by an aluminum can upon which is mounted a figured mask for obtaining a deposition rate gradient in the vertical direction (Fig. 2). This aluminum fixture is lined on the inside with aluminum foil, which flexes slightly with the accumulated film to further reduce flaking. A base vacuum pressure of $\sim 5\times 10^{-9}$ Torr is achieved by using a CTI-10 cryogenic pump. Process gas pressure is monitored with a capacitance manometer, with a variable position valve as the process gas pressure output control. Sputtering voltage, current, and process gas flow are monitored to provide an indication of target oxidation, outgassing, flaking, or other fault events during sputtering.

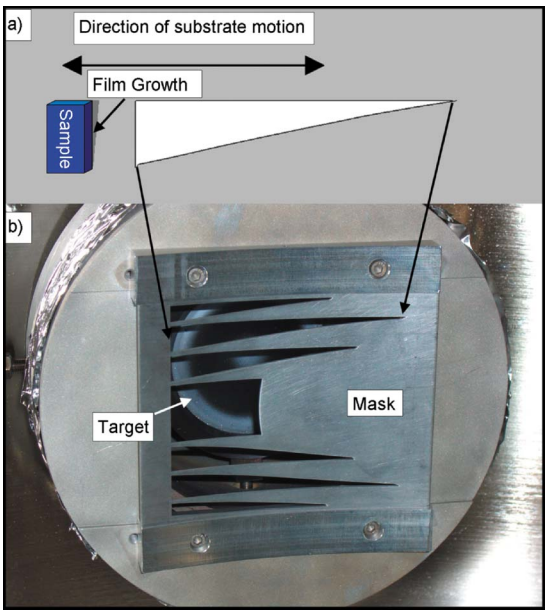

FIG. 2. (Color online) (a) Schematic of single-gradient mask used to produce the lateral deposition rate. (b) Photo of multiple-gradient mask with the WSi_2 sputtering target located behind. Each triangular tooth creates a lateral gradient across one Si substrate so that six samples may be grown simultaneously with this mask. The center of the aperture is used to grow a uniform film for growth rate analysis.

Si(100) substrates of 0.5–4.5 mm thickness are mounted in a vertical orientation on one of six facets available on a 200 mm diameter central drum and rotated back and forth in front of each gun for layer growth. The substrate to target distance is ~70 mm, with the sputtering flux width varying across each substrate from 0 up to ~60 mm through a shaped aperture discussed in more detail below. Both WSi_2 and Si sputtering takes place at an Ar pressure of 2.3 mTorr with a constant power of 215 W.[9–11] At areas where the shaped aperture is 15 mm wide to allow for a 15 mm sputtering flux width, the Si film growth rate is 1.0–1.3 nm/s, and the WSi_2 film growth rate is 3.0–4.0 nm/s. The WSi_2 target is 99.5% pure powder hot pressed with a bulk density of 8.10 g/cm^3, and the Si target is 99.999% pure and boron doped to allow for dc sputtering. No electrical bias is applied, nor is active heating or cooling presently applied to the substrates; however, the substrate temperature does rise somewhat above ambient due to the presence of the plasma and energetic ion bombardment. Optimization of these deposition parameters is the subject of an ongoing study.

A single layer is grown after first igniting the plasma while the substrates are outside the sputtering flux region. After the plasma has stabilized (7 s is typical for our configuration), the substrates are passed back and forth over the sputtering flux in order to build up the layer. Layer thickness is a function of drum angular velocity and number of passes over the sputtering gun. Custom software controls[12,13] ensure that each pass over the sputtering gun deposits ~5 Å of film growth. Thicker films are grown by passing the substrate over the sputtering flux more times or by modifying the angular velocity of the drum. In this manner, the monotonically increasing layer thicknesses required for wMLL (and MLL) growth are created by slight reductions in angular velocity.

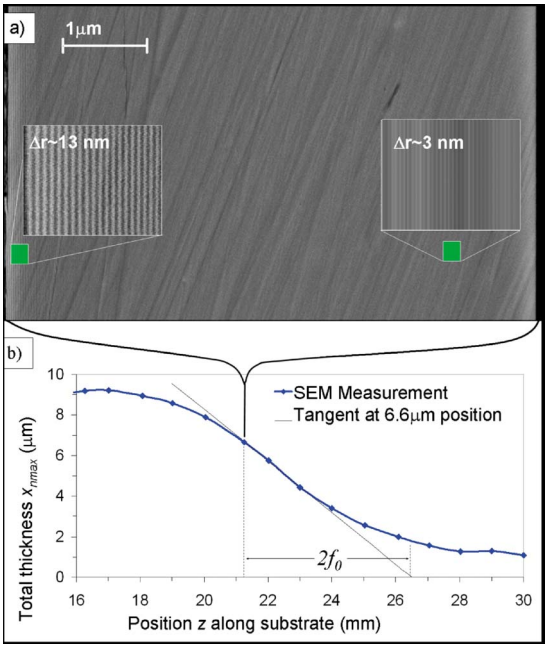

FIG. 3. (Color online) (a) SEM image of the 6.6 μm thick region of the wMLL. The diagonal striations are damage generated during dicing and polishing of the wMLL section. (b) Total structure thickness as a function of the z position along the sample as obtained from multiple SEM image analyses (the curve is merely a guide to the eye). The linear tangent shows the extrapolated intersection of all the layers at the 6.6 μm thick region, which should be at $2f_0$.

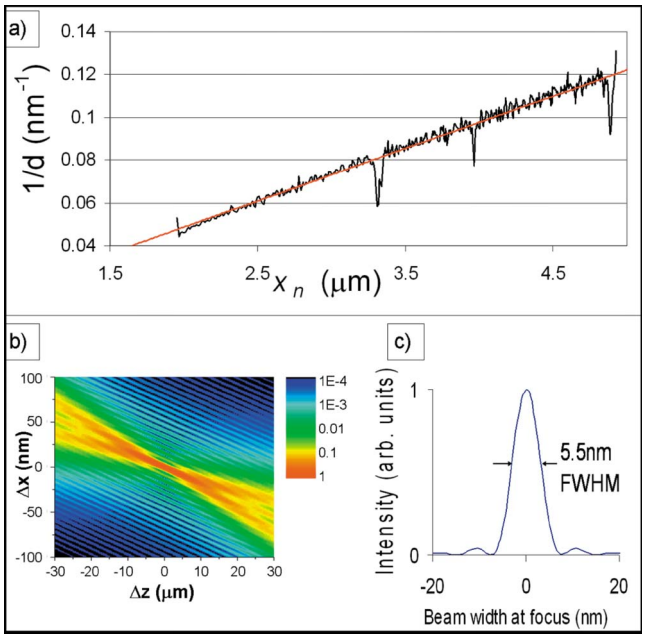

FIG. 4. (Color online) (a) Layer spacing profile obtained from analysis of the SEM image from Fig. 3, plotted as $1/d$ vs x_n. The large downward spikes are due to layer separation from polishing damage. (b) Simulated and normalized intensity contours (isophotes) in the focus region for a 30 mm thick section with the layer spacing profile shown by the linear fit in (a) at 82.1 keV. (c) The simulated intensity profile at the focus, with a FWHM of 5.5 nm and efficiency of 36.6% (Ref. 17).

The lateral gradient in the layer thicknesses is produced using a technique called profile coating.[14–16] By occluding part of the sputtering flux using a figured mask attached to the face of the sputtering gun cans, a deposition rate gradient can be produced along the direction perpendicular to the translation of the substrate. Due to the extreme lateral gradient required for these devices, the profile of the mask takes the shape of an acute triangle (see Fig. 2). Growth of nonlinear gradients can also be achieved by using a different mask.

Our proof-of-concept wMLL sample consists of 1588 alternating layers of WSi_2 and Si. The total deposition thickness ranges between 1 and 9 μm thick across an 11 mm long span of the substrate (Fig. 3), with the thickness at the most linear region being 6.6 μm. The layer thicknesses at this position increase monotonically according to Eq. (2), starting from 2.5 nm and ending at 13 nm. After growth, the wMLL sample was diced parallel to the lateral gradient direction and side polished.[8] A scanning electron microscopy (SEM) image of the 6.6 μm thick region of this structure is shown in Fig. 3(a). Figure 4(a) shows the inverse of the d-spacing as a function of position through the multilayer thickness extracted from SEM images at the 6.6 μm thick region. For a layer thickness sequence satisfying Eq. (2), the inverse d-spacing should vary with x_n as $d^{-1}=(2\Delta x_n)^{-1}=x_n/\lambda f_0$. The linear fit to the data shows that the zone plate law is satisfied by the deposited layers. From the measured lateral thickness gradient shown in Fig. 3(b), by using Eq. (4), we obtain an optimum focal length of 2.6 mm. From the inverse d-spacing fit in Fig. 4(a), we obtain a product $\lambda f_0=3.9\times10^{-14}$ m^2. The optimum wavelength for this lateral gradient and layer thickness sequence is thus $\lambda=0.0151$ nm, or a photon energy of 82.1 keV. Using the linear fit from Fig. 4(a) and dynamical diffraction theory for MLL structures,[7] the calculated intensity contours (isophotes) around the first-order focus are shown in Fig. 4(b). An intensity profile through the region of maximum intensity, shown in Fig. 4(c), yields an expected line focus full width at half maximum (FWHM) of 5.5 nm.[17] It is important to emphasize that this line focus is calculated from just the 39% of a complete wMLL structure represented by the layers shown in Fig. 4(a). An integrated efficiency of 36% has been simulated for this device with a 30 μm section depth.

To fabricate a wMLL for a particular x-ray wavelength, the multilayer must be sectioned at the correct z position so that the in-plane gradient matches the focal length of the layer sequence. This differs from flat or tilted MLLs, which can be sectioned at any position. However, wMLL structures show some tolerance to the energy deviation, from the optimum value. Within a small energy deviation, the focusing performance of wMLLs is not degraded significantly, as simulated using dynamical diffraction theory. If we were to section a 30 μm depth wMLL from the sample in Fig. 3(b) at the position where the total thickness is 6.6 μm, simulations[17] indicate that the focal spot size would be approximately constant within $\pm10\%$ of the optimum energy (82.1 keV). Lower-energy devices will have a smaller energy bandwidth.

ACKNOWLEDGMENTS

We thank Ralu Divan and Leo Ocola for their assistance with SEM imaging. This work was supported by the U.S. Department of Energy, Office of Science, Office of Basic Energy Sciences, under Contract No. DE-AC02-06CH11357.

[1] O. Hignette, P. Cloetens, G. Rostaing, P. Bernard, and C. Morawe, Rev. Sci. Instrum. **76**, 063709 (2005).
[2] H. Mimura, H. Yumoto, S. Matsuyama, Y. Sano, K. Yamamura, Y. Mori, M. Yabashi, Y. Nishino, K. Tamasaku, T. Ishikawa, and K. Yamauchi, Appl. Phys. Lett. **90**, 051903 (2007).
[3] C. Schroer and B. Lengeler, Phys. Rev. Lett. **94**, 054802 (2005).
[4] J. Maser, G. B. Stephenson, S. Vogt, W. Yun, A. Macrander, H. C. Kang, C. Liu, and R. Conley, Proc. SPIE **5539**, 185 (2004).
[5] H. C. Kang, J. Maser, G. B. Stephenson, C. Liu, R. Conley, A. T. Macrander, and S. Vogt, Phys. Rev. Lett. **96**, 127401 (2006).
[6] C. G. Schroer, Phys. Rev. B **74**, 033405 (2006).
[7] H. Yan, J. Maser, A. T. Macrander, Q. Shen, S. Vogt, G. B. Stephenson, and H. C. Kang, Phys. Rev. B **76**, 115438 (2007).
[8] H. C. Kang, G. B. Stephenson, C. Liu, R. Conley, R. Khachatryan, M. Wieczorek, A. T. Macrander, H. Yan, J. Maser, J. Hiller, and R. Koritala, Rev. Sci. Instrum. **78**, 046103 (2007).
[9] R. Conley, C. Liu, C. M. Kewish, A. T. Macrander, and C. Morawe, Proc. SPIE **6705**, 670505 (2007).
[10] C. Liu, R. Conley, A. T. Macrander, T. J. Graber, C. Morawe, C. Borel, and E. M. Dufresne, Proc. SPIE **5537**, 154 (2004).
[11] C. Liu, R. Conley, A. T. Macrander, J. Maser, H. C. Kang, M. A. Zurbuchen, and G. B. Stephenson, J. Appl. Phys. **98**, 113519 (2005).
[12] R. Conley, C. Liu, and A. T. Macrander, "Deposition system control program," Software copyright, 2006.
[13] R. Conley, C. Liu, and A. T. Macrander, "Multilayer Laue lens sequence compiler," Software copyright, 2006.
[14] C. Liu, R. Conley, A. T. Macrander, and L. Assoufid, J. Vac. Sci. Technol. A **21**, 1579 (2003).
[15] W. C. Sweatt, U.S. Patent No. 5948468 (1999).
[16] J. R. Kurdoch and R. R. Austin, Phys. Thin Films **10**, 261 (1978).
[17] H. Yan, H. C. Kang, J. Maser, A. T. Macrander, C. M. Kewish, C. Liu, R. Conley, and G. B. Stephenson, Nucl. Instrum. Methods Phys. Res. A **582**, 126 (2007).